

# Biofilter CFD Modeling for Atmospheric Emissions Control of a Heating System Based on Sawdust Pellets

Fidel Vallejo<sup>a,\*</sup>, Serguei Alejandro-Martin<sup>a</sup>, Camilo Díaz<sup>b</sup>, Luis Díaz-Robles<sup>c</sup>, Diana Yáñez-Sevilla<sup>c</sup>, Catalina Del Campo<sup>d</sup>

<sup>a</sup>Wood Engineering Department, Engineering Faculty, Universidad del Bío-Bío, Concepción, Chile.

<sup>b</sup>Mechanical Engineering Department, Engineering Faculty, Universidad del Bío-Bío, Concepción, Chile.

<sup>c</sup>Chemical Engineering Department, Universidad de Santiago de Chile, Santiago, Chile.

<sup>d</sup>Department of Civil Engineering, Universidad Técnica Federico Santa María, Valparaíso, Chile.

[fvallejo@ubiobio.cl](mailto:fvallejo@ubiobio.cl)

The use of waste biomass, e. g., sawdust, is an alternative for heating and industry in countries with large areas of radiata pine and eucalyptus forests. Indeed, the Chilean demand for domestic, industrial, and district heating has been increasing in recent years, standing at 75 kt/y and increasing by 400 % until 2030. However, burning hydrophilic sawdust pellets and wooden logs generates particle matter, NO<sub>x</sub>, and polycyclic aromatic hydrocarbons (PAHs) emissions that have placed this fuel as one of the most contributing pollutants to the atmosphere in southern Chile. According to current emission inventories, residential biomass combustion contributed more than 95 % of total particulate matter emissions. It has become a limitation for biomass as a source of energy and a challenge for applying Waste-to-Energy technologies to obtain biochars with greater calorific value and less ash. On the other hand, PAHs are the most problematic pollutants group to reduce in the solid and gas phase due to their high molecular weight. It is essential to study a system that diminishes those pollutants by improving the solid fuel and the pellet stove and developing an efficient pollution control system, like a PAHs biofilter. This research studied the emission of benzo(a)pyrene, a model compound of PAHs, during the combustion of commercial pellets in a stove. The PAHs emissions, determined by gas chromatography, were between 17.8 and 22.4 µg/kg of pellets with an operating temperature range of 350 to 450 °C. A biofiltration system treated the exit combustion gas for pollutant abatement. Vermiculite was used as a support medium coated with a microbial consortium composed of *Fusarium solanis* and *Rhodococcus erythropolis*. The system showed an efficiency of nearly 70 % and an elimination capacity of 250 µgm<sup>-3</sup>h<sup>-1</sup>. On the other hand, for the CFD modeling, the geometry was obtained by a mathematical algorithm of random generation for packed beds in bioreactors. The model meshing and numerical solution were carried out in OpenFOAM, with the solvers SimpleFoam and scalarTransportFoam. The resolution of the velocity-pressure field using SimpleFOAM showed a maximum error of 6.1 %, and for the concentration of the pollutant, the error was 6.2 %.

## 1. Introduction

In Chile, environmental problems are mainly related to emissions from mobile and industrial sources and the use of firewood for home heating. In indoor air, there is the presence of pollutants, not only due to the entry of outside air but also due to human activity that produces CO<sub>2</sub>, construction materials that generate particulate matter, and cleaning products whose composition contains organic solvents. In addition, the incomplete combustion of biomass (mainly firewood) for heating generates a high presence of polycyclic aromatic hydrocarbons (PAHs) (Pozo et al., 2015). These pollutants cause toxic effects such as respiratory diseases and cancer and affect the nervous and immune systems (Guiyusse et al., 2008). These harmful effects on health can be mitigated by eliminating pollutants in indoor air, and biofiltration systems have been used for this in recent years due to the advantages they present: relative simplicity of operation, low maintenance costs, investment, and extensive experience gained in its design and operation (Estrada et al., 2013). Biofilters have been

developed that eliminate between 70 to 90 % of specific pollutants such as formaldehyde (Shao et al., 2020) and VOCs (Guieysse et al., 2008), among others. However, PAHs (Trojanowicz, 2020) have not been worked on before. In this work, the main operational parameters of a biofiltration system that allows the abatement of benzo[a]pyrene as a model compound of PAHs, using colonies of bacteria and filamentous fungi, were determined. The emission factors were obtained by gas chromatography, and the efficiency was validated with a CFD simulation.

## 2. Methodology

### 2.1 Experimental setup

The evaluated combustion system corresponds to the controlled burning of sawdust pellets (Pinus radiata) in a JSR brand stove with 1.4 kW of power, which allows a maximum temperature of 1,000 °C. The pellets were burned at 350 to 450 °C to simulate actual domestic operating conditions. The exhaust gases entered a 32 W Hailea brand compressor with a capacity of 60 L/min. The compressor outlet stream was fed to a mixing chamber, where fresh air was incorporated, and a rotameter controlled the flow. The abatement scheme was a biofiltration system described in detail in the following sections. Figure 1 shows the system operation diagram. The dry air (20 % relative humidity) is humidified up to 60 – 70 % to recreate the environmental conditions in the southern areas of Chile. The air with benzo(a)pyrene (BaP) was fed to a biofilter in the bottom stage. The biofilter has a pressure control system and a stream of nutrients for the bacterial-fungal consortium. Finally, the outlet gas flow is measured with a rotameter, and samples are taken for chromatographic analysis.

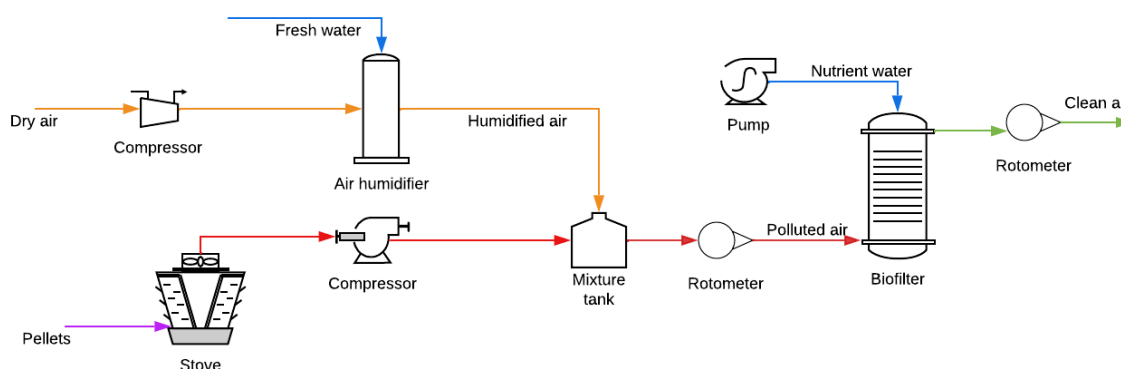


Figure 1: Experimental setup of Benzo(a)pyrene generation and abatement system

The biofilter used to remove contaminants in the gas phase consists of three stages, each with a vermiculite bed (> 4 mesh) covered with a microbial consortium formed by *Fusarium solanis* and *Rhodococcus erythropolis*. The bed height in each stage is 25.0 cm, with an inner diameter of 8 cm. The operation of the biofilters is reported by determining two parameters: removal capacity and efficiency. The removal capacity is defined as the absolute mass quantity of contaminant that the biofilter can remove per unit of time and volume of the biofilter Eq(1). Efficiency is the relative percentage of a pollutant removed concerning the initial load, the latter being the amount of contaminant that enters the biofilter with the air Eq(2).

$$RC = \frac{Q(C_{gi} - C_{go})}{V_r} \quad (1)$$

$$\eta = \frac{C_{gi} - C_{go}}{C_{gi}} \times 100 \quad (2)$$

Where,  $\varepsilon$  is the biofilter efficiency, RC is the removal capacity (g/m<sup>3</sup>h), Q is the volumetric flow (m<sup>3</sup>/h),  $V_r$  is the empty-bed biofilter volume,  $C_{gi}$  and  $C_{go}$  are the pollutant concentration at inlet and outlet.

### 2.2 Biological agents for the abatement of Benzo(a)pyrene

The biological agent used for biofiltration is a microbial consortium composed of the filamentous fungus *Fusarium solani* and the bacterium *Rhodococcus erythropolis*. The process of inoculation and culture of the consortium is described in (Vergara-Fernández et al., 2018). The support material used as packing for the

biofiltration column was a mineral called vermiculite. Among its main properties, it stands out that it has low density, is inert, neutral, highly absorbent, and has a pH of 7 (Rashad, 2016).

### 2.3 CFD Simulation Setup

The modeling geometry was constructed using the random packed column fill algorithm (Wang et al., 2022), with a nominal diameter of 4.8 mm (mesh 4). For processing the information in Paraview, the data generated by the algorithm was imported through a CSV (Comma Separated Value) text file. This file included four columns of variables: the location of the center of the sphere ( $x,y,z$ ) and  $r$  for the radius of each spherical particle. After importing the CSV file, each point was located within 3D space. The obtained sphere can be visualized in Figure 2a, and the group of spheres within the simulation domain is shown in Figure 2b. After generating the bed of spheres, the file is exported in STL (Standard Triangle Language) format. The three-dimensional body was processed in OnShape and meshed in SimFlow, before numerical resolution with the same software. The visualization of the results of the final results of the simulation was carried out in Paraview.

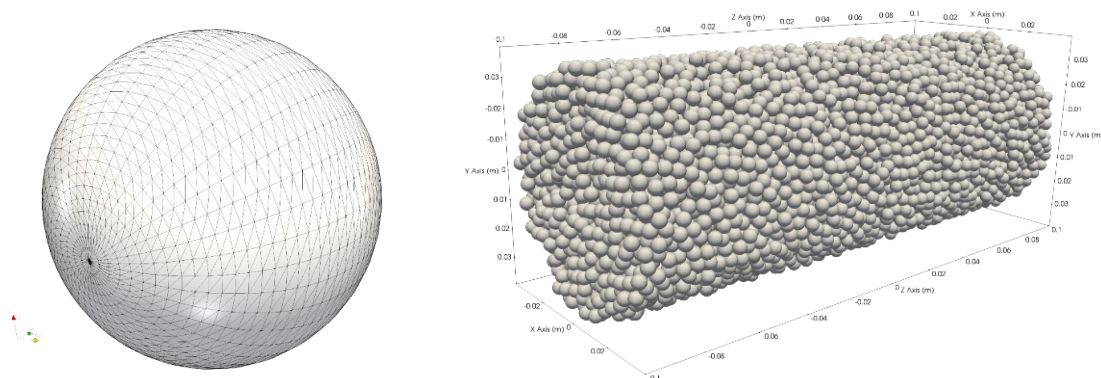


Figure 2: (a) sphere of support material, (b) packed bed of the biofilter

## 3. Results and discussions

### 3.1 Determination of biofilter system efficiency

Three samples of the biofilter inlet and outlet gas were taken under stable operating conditions: at the stove outlet and the biofilter inlet and outlet. All collections were made in triplicate, and the average value is indicated here. The emission of benzo(a)pyrene produced by the combustion of pellets fluctuated between 17.8 and 22.4 ug/kg between 350 and 450 °C. In the literature, there are not enough references to compare this emission value. The EPA AP-42 guide establishes a value of 0.020 lb/t for the 7-PAH set and 0.053 lb/t for the 16-PAH (EPA, 1995).

On the other hand, a study carried out in various Italian cities reported BaP emissions between 0.05 and 10 mg/kg (Gianelle et al., 2013). The value determined by this study could be used in successive emission inventories when a norm is established that regulates the generation of PAHs from biomass combustion. Finally, the efficiency of the biofiltration system was 70 %. The influence of the variation of the initial concentration of BaP was studied, controlled by dilution in the mixing chamber with fresh air for a total flow of 0.21 m<sup>3</sup>/h. The results are in Figure 3, where the straight regression line with a good fit indicates that the biofilter removes at a constant proportional rate in this range of initial concentrations. Finally, these concentrations cover a wide range of environmental concentrations caused by benzo(a)pyrene for indoor air and flows that come directly from the pellet combustion stove (Thompson et al., 2019).

### 3.2 CFD Simulation

The numerical resolution was performed using the SIMPLE method (**S**emi-**I**mplicit **M**ethod for **P**ressure-**L**inked **E**quations (Xiong et al., 2014). The general mass transfer equation is indicated in Eq(3). Fick's First Law establishes the relationship between the molar net flux and the diffusion coefficient, the rate of change of the concentration, and the molecular convective contribution, which is observed in Eq(4). If these equations are combined, Eq(5) and Eq(6) are obtained to describe the transient and steady-state of concentration change in the Cartesian axes of space. Eq(7) is a development from the nabla operator since, by default, OpenFOAM works three-dimensionally (Jasak, 2009). The consumption rate  $R$  of benzo(a)pyrene is described by the Monod equation Eq(8) (Zeng and Zhang, 2005).

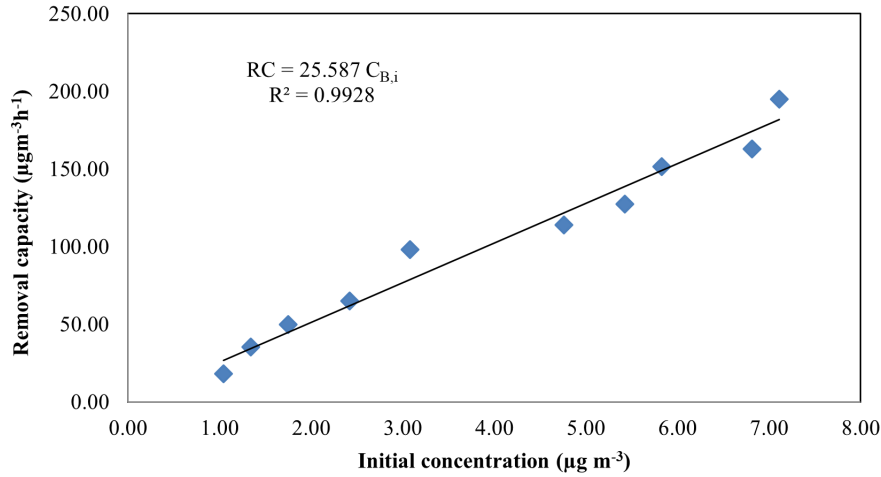


Figure 3: Benzo(a)pyrene Removal Capacity in terms of initial concentration

$$\nabla \cdot N_i - \frac{\partial C_i}{\partial t} - R_i = 0 \quad (3)$$

$$N_i = -D\nabla C_i + C_i V \quad (4)$$

$$-D\nabla^2 C_i + \frac{\partial C_i}{\partial t} + V \nabla C_i - R_i = 0 \quad (5)$$

$$-D\nabla^2 C_i + V \nabla C_i = 0 \quad (6)$$

$$-D \left( \frac{\partial^2 C_B}{\partial x^2} + \frac{\partial^2 C_B}{\partial y^2} + \frac{\partial^2 C_B}{\partial z^2} \right) + V \left( \frac{\partial C_B}{\partial x} + \frac{\partial C_B}{\partial y} + \frac{\partial C_B}{\partial z} \right) = 0 \quad (7)$$

$$R = v_{max} \frac{\frac{C}{H}}{K_S + \frac{C}{H}} \quad (8)$$

Where  $\nabla N_i$  is the molar flux,  $C_i$  is the molar concentration,  $R_i$  is the generation rate,  $D$  is the mass transfer diffusion coefficient,  $V$  is the orthogonal velocity,  $v_{max}$  is the maximum growth rate,  $K_S$  is the Monod constant - or half-velocity, and  $H$  is the Henry coefficient.  $B$  and  $i$  are for benzo(a)pyrene and specie  $i$ . The generated volume was meshed into 1.95 million cells using SimFlow. First, the pressure and velocity field were determined under laminar flow conditions for steady-state in each experimental condition: 0.21, 0.30, and 0.42 m<sup>3</sup>/h. For the boundary conditions, the initial velocity in the biofilter was determined with the area corrected by the porosity value, as observed in Eq(9).

$$v = \frac{Q}{A\varepsilon} \quad (9)$$

Where  $v$  is the average air inlet velocity in the cross-section of the base of the column (m/s),  $Q$  is the flow rate (m<sup>3</sup>/s),  $A$  is the cross-sectional area of the biofilter (m<sup>2</sup>), and  $\varepsilon$  is the void fraction, the experimental value for this work was 0.42. Table 1 contains the simulated pressure ranges within each stage of the biofilter when the airflow is 0.21 m<sup>3</sup>/h. The pressure drops and the range of velocities determined in the CFD simulations are also presented. The pressure drops in each stage were between 35 and 37 Pa, with velocities up to 0.146 m/s. Figure 4 presents the visualization of the pressure field in the three stages, where the pressure drop by regions inside the biofilter is noted, and an axial section of the column. The blue color corresponds to the zone with higher pressures, while the red zone corresponds to the lower pressure values when convergence in the result is reached. In the development of the velocity field, it can be concluded that the value is far from being constant in the radial direction, as is assumed when working with plug flow (Dabros et al., 2018). As expected, the zones with more available space show a greater flow development.

Table 1: CFD Numeric solution for biofilter – Pressure and velocity field

| Stage  | Description                     | Value        | Units |
|--------|---------------------------------|--------------|-------|
| First  | Pressure range (outlet – inlet) | 72.1 – 107.0 | Pa    |
|        | Pressure drop                   | 34.9         | Pa    |
|        | Magnitude velocity range        | 0 – 0.146    | m/s   |
| Second | Pressure range (outlet – inlet) | 37.1 – 72.1  | Pa    |
|        | Pressure drop                   | 35.0         | Pa    |
|        | Magnitude velocity range        | 0 – 0.146    | m/s   |
| Third  | Pressure range (outlet – inlet) | 0 – 37.1     | Pa    |
|        | Pressure drop                   | 37.1         | Pa    |
|        | Magnitude velocity range        | 0 – 0.146    | m/s   |

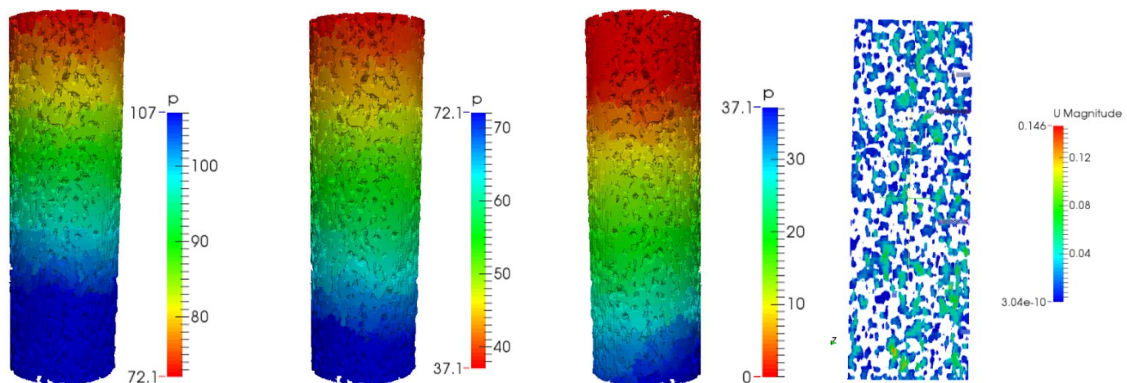


Figure. 4: Pressure and velocity fields in the biofilter

With the distribution of velocities and pressures in steady-state, a new phase of CFD simulations in transient state was initiated using the scalarTransportFoam solver. The concentrations at the outlet in each stage and for each of the flows studied were determined, and the efficiency was calculated with respect to the initial concentration of benzo(a)pyrene. In Figure 5, the modeled and experimental values for C1: 0.42 m<sup>3</sup>/h, C2: 0.30 m<sup>3</sup>/h and C3: 0.21 m<sup>3</sup>/h are indicated. The modeled efficiencies present a good fit with maximum errors of 6 %.

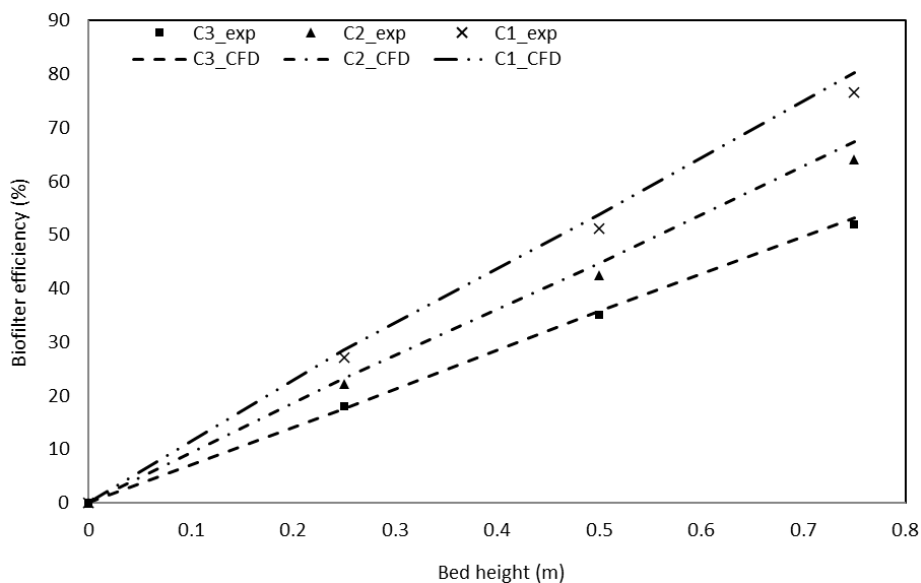


Figure. 5: CFD modeled and experimental efficiencies comparison

#### 4. Conclusions

This study analyzes the emission and control of a type of pollutant generated by the incomplete combustion of biomass. Benzo(a)pyrene was considered a model compound of the PAH group. In the first phase, it was experimentally determined that the emission was 17.8 to 22.4 µg/kg between 350 and 450 °C. The stove outlet gas was mixed with pure humidified air to regulate the ambient concentration value and simulate relative humidity values in southern Chile. The biofiltration system showed efficiencies greater than 70 %.

Finally, a CFD simulation of the complete biofilter was carried out for inlet air flows between 0.21 and 0.42 m<sup>3</sup>/h, and the pressure fields and velocity distribution inside it were obtained. The error calculated for the pressure drops concerning the experimental data is less than 5 %, which validates the velocities calculated by the software. For contaminant removal efficiency, the errors did not exceed 6 %, indicating that the Monod equation can describe the physical-chemical behavior of BaP in the microbial consortium and that future simulations can be developed to optimize the design of the biofiltration system. and improve efficiency.

#### References

- Dabros T.M.H., Stummann M.Z., Høj M., Jensen P.A., Grunwaldt J.D., Gabrielsen J., Mortensen P.M., Jensen A.D., 2018, Transportation fuels from biomass fast pyrolysis, catalytic hydrodeoxygenation, and catalytic fast hydrolysis, *Progress in Energy and Combustion Science*, 68, 268–309. DOI: 10.1016/J.PECS.2018.05.002.
- EPA, 1995. Appendix B Documentation of 7-PAH and 16-PAH National Emission Estimates. In *Compilation of Air pollutant Emission factors: Vol. I.* <[https://www3.epa.gov/airtoxics/112c6/app\\_b.pdf](https://www3.epa.gov/airtoxics/112c6/app_b.pdf)>, accessed 15.06.2022.
- Estrada J.M., Hernández S., Muñoz R., Revah S., 2013. A comparative study of fungal and bacterial biofiltration treating a VOC mixture. *Journal of Hazardous Materials*, 250–251, 190–197. DOI: 10.1016/j.jhazmat.2013.01.064.
- Gianelle V., Colombi C., Caserini S., Ozgen S., Galante S., Marongiu A., Lanzani G., 2013. Benzo(a)pyrene air concentrations and emission inventory in Lombardy region, Italy. *Atmospheric Pollution Research*, 4(3), 257–266. DOI: 10.5094/APR.2013.028.
- Guieysse B., Hort C., Platel V., Munoz R., Ondarts M., Revah S., 2008. Biological treatment of indoor air for VOC removal: Potential and challenges. *Biotechnology Advances*, 26(5), 398–410.
- Jasak H., 2009. OpenFOAM: Open source CFD in research and industry. *International Journal of Naval Architecture and Ocean Engineering*, 1(2), 89–94. DOI: 10.2478/IJNAOE-2013-0011.
- Pozo K., Estellano V.H., Harner T., Diaz-Robles L., Cereceda-Balic F., Etcharren P., Pozo K., Vidal V., Guerrero F., Vergara-Fernández A., 2015. Assessing Polycyclic Aromatic Hydrocarbons (PAHs) using passive air sampling in the atmosphere of one of the most wood-smoke-polluted cities in Chile: The case study of Temuco. *Chemosphere*, 134, 475–481. DOI: 10.1016/j.chemosphere.2015.04.077.
- Rashad A.M., 2016. A synopsis about perlite as building material – A best practice guide for Civil Engineer. *Construction and Building Materials*, 121, 338–353, DOI: 10.1016/j.conbuildmat.2016.06.001.
- Shao Y., Wang Y., Zhao R., Chen J., Zhang F., Linhardt R.J., Zhong W., 2020. Biotechnology progress for removal of indoor gaseous formaldehyde. *Applied Microbiology and Biotechnology*, 104(9), 3715–3727. DOI: 10.1007/S00253-020-10514-1.
- Thompson V.S., Ray A.E., Hoover A., Emerson R., Hartley D., Lacey J.A., Yancey N., Thompson D.N., 2019. Assessment of municipal solid waste for valorization into biofuels. *Environmental Progress & Sustainable Energy*. DOI: 10.1002/ep.13290.
- Trojanowicz M., 2020. Removal of persistent organic pollutants (POPs) from waters and wastewaters by the use of ionizing radiation. *Science of the Total Environment*, 718, DOI: 10.1016/J.SCITOTENV.2019.134425.
- Vergara-Fernández A., Yáñez D., Morales P., Scott F., Aroca G., Diaz-Robles L., Moreno-Casas P., 2018. Biofiltration of benzo[*a*]pyrene, toluene and formaldehyde in air by a consortium of *Rhodococcus erythropolis* and *Fusarium solani*: Effect of inlet loads, gas flow and temperature. *Chemical Engineering Journal*, 332, 702–710. DOI: 10.1016/J.CEJ.2017.09.095.
- Wang X., Yin Z.Y., Su D., Wu X., Zhao J., 2022. A novel approach of random packing generation of complex-shaped 3D particles with controllable sizes and shapes. *Acta Geotechnica*, 17(2), 355–376. DOI: 10.1007/S11440-021-01155-3/FIGURES/24.
- Xiong Q., Aramideh S., Passalacqua A., Kong S.C., 2014. BIOTC: An open-source CFD code for simulating biomass fast pyrolysis. *Computer Physics Communications*, 185(6), 1739–1746. DOI: 10.1016/j.cpc.2014.02.012.
- Zeng H., Zhang T.C., 2005. Evaluation of kinetic parameters of a sulfur–limestone autotrophic denitrification biofilm process. *Water Research*, 39(20), 4941–4952. DOI: 10.1016/j.watres.2005.09.034.